ISSN 1063-7850, Technical Physics Letters, 2008, Vol. 34, No. 9, pp. 768–770. © Pleiades Publishing, Ltd., 2008.
Original Russian Text © L.A. Dar'yan, A.P. Drozhzhin, S.M. Korobeĭnikov, V.S. Teslenko, M.A. Anikeeva, 2008, published in Pis'ma v Zhurnal Tekhnicheskoĭ Fiziki, 2008, Vol. 34, No. 17, pp. 88–94.

Detecting Microbubbles in Transformer Oil

L. A. Dar'yan[a]*, A. P. Drozhzhin[b], S. M. Korobeĭnikov[b], V. S. Teslenko[b], and M. A. Anikeeva[b]

[a] *Novosibirsk State Technical University, Novosibirsk, Russia*

[b] *Lavrentiev Institute of Hydrodynamics, Siberian Branch, Russian Academy of Sciences, Novosibirsk, Russia*

**e-mail: ldarian@mail.ru*

Received January 10, 2008

Abstract—The growth of microbubbles under the action of a negative pressure wave in transformer oil (TO) has been studied. It is established that microbubbles in TO grow to a detectable size of 100–200 μm. According to the results of calculations, these bubbles can develop from the nuclei of micron and submicron dimensions.

PACS numbers: 77.84.Nh, 47.55.D

DOI: 10.1134/S1063785008090150

The assumption concerning the existence of microbubbles and/or their formation under the action of electric field is important in explaining the mechanism of pulsed electric breakdown in liquid media [1]. It was experimentally established that micron-sized bubbles always exist in water [2]. The hypothesis that such microbubbles are also present in transformer oil (TO) was also repeatedly formulated, but no convincing experimental evidence in favor of or against this hypothesis has been reported so far.

In this study, we have attempted at experimentally detecting the presence and evaluating the size of microbubbles in commercial TO samples of different purity grades using a method described previously [3].

The experimental method is based on the phenomenon of increase in the size of bubbles in a liquid under the action of a negative pressure wave. According to this, bipolar shock waves were generated in TO by an electromagnetic source. Being reflected from a free surface, these waves created reduced pressure that was sufficient for the development of cavitation in this liquid medium.

Figure 1 shows a schematic diagram of a probed cylindrical region in the TO, where size a is determined by the depth of focus of an optical system and size b, by the diameter of the objective diaphragm in this system. Thus, the cylinder under consideration is a region of the best focus, the depth of which was established using the image of a thin wire (with a diameter of 0.14 mm) moved by a high-precision screw drive. This region was situated at a depth of 20 mm from the TO surface.

The probed region was illuminated from the left side by the light of a pulsed lamp (ISSh 400-3) with a pulse duration of 1 μs via a diffuse thin-film screen, which ensured uniform illumination of the TO volume. The lamp discharge start moment t_d was controlled using a pulse delay generator (GZI-6). The optical detection system was positioned on the right of the TO volume and comprised a digital photo camera (Canon PowerShot S21S with 5×10^6 pixels) and a lens system. The image pixel size corresponded to approximately 3 μm-sized element of the object. The pressure in the probed region was measured by a piezoelectric sensor with the temporal and spatial resolution of 0.05 μs and 0.5 mm, respectively.

The experiments were performed with samples of a fresh TO (GK grade) and a model TO–sand mixture. All samples were characterized in terms of the commercial purity grade (CPG) using a standard device of the AZZh-975 type. We have studied two batches of pure TO and prepared two batches of the TO–sand mixture as follows. A weighed amount of quartz sand was added to a given volume of TO, after which the mixture was vigorously shaken and allowed to stand for 24 h.

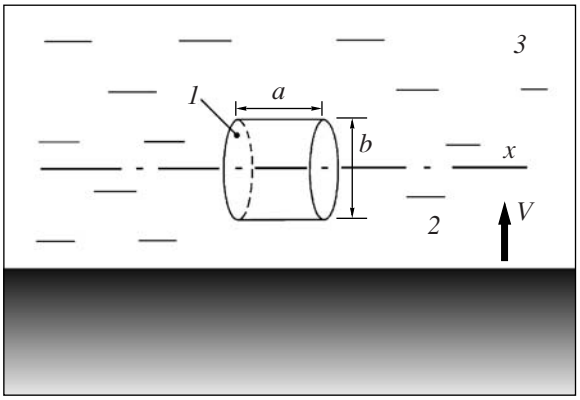

Fig. 1. Schematic diagram of the experimental arrangement: (*1*) probed region of TO (a = 1.95 ± 0.05 mm; b = 1.64 ± 0.1 mm); (*2*) shock wave front; (*3*) volume filled with TO; (x) optical axis; (V) shock wave velocity vector.

Table 1. Results of particle size analysis in pure TO (GK grade, batch 1) (V = 100 ml, CPG = 8)

2–5 μm	5–10 μm	10–25 μm	25–50 μm	50–100 μm	>100 μm
72093	4919	1131	118	53	2

Table 2. Results of particle size analysis in pure TO (GK grade, batch 2) (V = 50 ml (×2), CPG = 8)

2–5 μm	5–10 μm	10–25 μm	25–50 μm	50–100 μm	>100 μm
34264	3588	928	130	62	10

Table 3. Results of particle size analysis in TO–sand mixture prepared from 450 ml GK-grade oil and 115 ml of sand (V = 100 ml, CPG = 13)

2–5 μm	5–10 μm	10–25 μm	25–50 μm	50–100 μm	>100 μm
31267	133751	23831	334	82	4

Table 4. Results of particle size analysis in TO–sand mixture prepared from 300 ml GK-grade oil + 100 ml of sand (V = 100 ml, CPG = 13)

2–5 μm	5–10 μm	10–25 μm	25–50 μm	50–100 μm	>100 μm
38446	162367	29664	346	45	11

Then the supernatant fraction was thoroughly decanted into the experimental cell.

The results of particle size analysis and CPG determination of the TO samples are given in Tables 1–4. As can be seen from Tables 1 and 2, fresh (neither used nor additionally purified) commercial TO has CPG = 8, while the TO–sand mixtures after standing for two days had CPG = 13. Note that the TO–sand mixtures were characterized by a significantly greater content of small particles belonging to 5–25 μm fractions (fractions below 2–5 μm were not analyzed).

The development of microbubbles was studied in TO samples of three types: TO–sand mixture (sample 1), initial ("pure") TO (sample 2), and pure TO saturated with air by bubbling for 60 min. Several series of photographs of cavitation microbubbles were obtained for various delay times t_d, each series including up to 20 images. The probing pulse delay time was determined relative to the shock wave start. The maximum number of photographs was obtained for t_d = 50.4 μs, which corresponded to the maximum probability of cavitation bubble formation.

Figure 2 shows the typical pressure waveforms in the vicinity of the probed region and the corresponding photographs of cavitation bubbles in the TO with suspended small fraction of particles (sample 1). As can be seen from Fig. 2a, the amplitude of rarefaction wave *1* at t_d = 48 μs is greater than that of wave *2*, which implies that an increase in the shock wave energy is accompanied by distortion of the rarefaction wave. This is related to the development of cavitation bubbles, which disturb the real pressure field in the probed region. The effect of cavitation bubbles on the pressure amplitude was minimized by selecting appropriate shock wave energy. The number of bubbles per unit volume, which was determined using photographs and calculated taking into account the size of a probed region, amounted to 1214 cm^{-3} (Fig. 2b) and 728 cm^{-3} (Fig. 2c).

For TO samples 2 and 3, the photographs did not reveal clear cavitation bubbles in the probed region, but some images contained poorly focused, smeared objects. From this we may conclude that microbubbles also exist in pure oil, but their concentration (approximately, below 100 cm^{-3}) is insufficient to provide for their reliable detection.

Since the bubbles observed in our experiments grew from smaller nuclei, we attempted to reconstruct their initial size by solving the following differential equation:

$$R\frac{d^2R}{dt^2} + \frac{3}{2}\left(\frac{dR}{dt}\right)^2 + \frac{4}{\rho}\frac{\eta}{R}\frac{dR}{dt} + \frac{2}{\rho}\frac{\sigma}{R} = \frac{1}{\rho}(P_{in} - P_{out}),$$

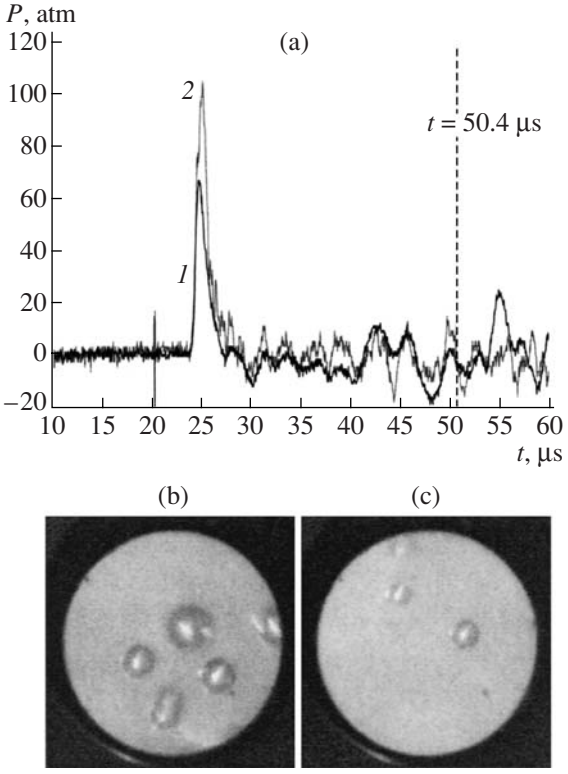

Fig. 2. (a) The typical pressure waveforms in the probed region for different shock wave amplitudes and (b, c) photographs of cavitation bubbles in the TO–sand mixture in two experiments with a minimum amplitude of the rarefaction wave at t_d = 50.4 μs.

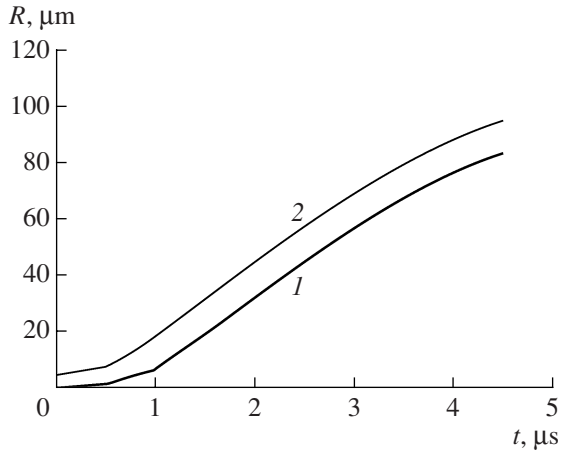

Fig. 3. Calculated dependence of cavitation bubble radius on the time for the nucleus radius of (*1*) 0.5 μm and (*2*) 5 μm.

where R is the current radius of a bubble; ρ, η, and σ are the density, viscosity, and surface tension of the liquid, respectively; P_{in} is the internal pressures in the bubble; and P_{out} is the pressure outside the bubble. The real waveform of a pressure wave (Fig. 2a) was replaced by an idealized profile, according to which the external pressure decreased to –1.1 MPa for 2 μs, then restored on a zero level within 2 μs, and remained constant for 2.4 μs (up to detection time).

Figure 3 shows the results of calculations of the bubble growth dynamics. As can be seen, the growth rate is small as the initial stage (where the surface tension plays a significant role) and after termination of the negative pressure pulse (where the bubble grows by inertia). An interpolation of the size of detected bubbles to the calculated values of nuclei, from which they have developed, leads to a conclusion that the observed bubbles arise from the nuclei of micron and submicron dimensions that existed in TO prior to the arrival of the negative pressure wave.

In conclusion, we have performed for the first time experimental investigations that show evidence for the existence of microbubbles of both micron and submicron dimensions in TO. It is shown that the number of microbubbles in TO strongly depends on the presence of "mechanical" contaminations. In TO with CPG = 8, the concentration of microbubbles is apparently below 100 cm^{-3}, whereas in TO with CPG = 13, their concentration is reliably detected on a level of 1000 cm^{-3}.

REFERENCES

1. V. Ya. Ushakov, V. F. Klimkin, S. M. Korobeinikov, and V. V. Lopatin, in *Breakdown of Liquids under Pulse Voltage* (NTL, Tomsk, 2005) [in Russian].
2. A. S. Besov, V. K. Kedrinskiĭ, and E. I. Pal'chikov, Pis'ma Zh. Tekh. Fiz. **15** (16), 23 (1989) [Tech. Phys. Lett. **15**, 630 (1989)].
3. G. N. Sankin and V. S. Teslenko, Dokl. Akad. Nauk **393**, 762 (2003) [Dokl. Phys. **48**, 665 (2003)].

Translated by P. Pozdeev